Inorg. Chem. **2006**, *45*, 5417−5428

Models of the Cytochromes: Crystal Structures and EPR Spectral Characterization of Low-Spin Bis-Imidazole Complexes of (OETPP)Fe^{III} Having Intermediate Ligand Plane Dihedral Angles

Liliya A. Yatsunyk, Alice Dawson,† Michael D. Carducci, Gary S. Nichol, and F. Ann Walker*

Department of Chemistry, University of Arizona, Tucson, Arizona 85721-0041

Received February 18, 2006

The preparation, EPR spectra, and crystal structures of octaethyltetraphenylporphyrinatoiron(III) having two imidazole, *N*-benzylimidazole, and *N*-methylimidazole axial ligands are reported, [(OETPP)Fe(HIm)$_2$]Cl, [(OETPP)Fe(N-BzIm)$_2$]-Cl, and [(OETPP)Fe(N-MeIm)$_2$]Cl. Despite large variation in axial ligand size, the unit cell parameters for all complexes are very similar; each structure has the same basic motif, with large voids formed by the extended porphyrin framework (filled by ordered or disordered axial ligands and disordered solvent), which allows differently sized ligands to fit within the same cell dimensions. Each porphyrin core adopts a saddled conformation with $|\Delta C_\beta| =$ 1.13–1.15 Å. The dihedral angles between axial ligand planes, $\Delta\varphi$, are far from being either ideal parallel or perpendicular: 30.1°, 57.2° for [(OETPP)Fe(HIm)$_2$]Cl (molecules **1** and **2**), 56.8° for [(OETPP)Fe(N-BzIm)$_2$]Cl, and 16.0°, 44.6°, 59.6°, and 88.1° for [(OETPP)Fe(N-MeIm)$_2$]Cl, which has disordered axial ligands. Among the complexes of this study, an axial ligand $\Delta\varphi$ of 56.8° is found to be the largest "parallel" angle (as defined by the observation of a normal rhombic or Type II EPR signal (N-BzIm, $g = 3.08, 2.19, 1.31$)), while 57.2° is found to be the smallest "perpendicular" $\Delta\varphi$ (as defined by the observation of a "large g_{max}" or Type I EPR signal (HIm, $g_{max} = 3.24$)). From the results of this study, it is clear that the size of the largest *g* for Types I and II complexes varies continuously, with no break between the two. While the switch in EPR signal type, from Type II to Type I, appears to be very sharp in this study, this may be somewhat artificial based upon limited numbers of examples and the required saddle distortion of the (OETPP)Fe^{III} complexes. However, in comparison to several proteins with dihedral angles near 60° and Type II EPR spectra, we may conclude that the switch in EPR signal type occurs near 57° ± 3–5°.

Introduction

Bis-imidazole and bis-pyridine complexes of Fe^{III} porphyrins,[1−3] including the octaalkyltetraphenylporphyrins[3,4] provide excellent models for bis-histidine coordinated heme centers involved in a number of cytochrome-containing systems, examples of which include cytochromes *b* of mitochondrial Complexes II[5] and III[6−20] and of chloroplast cytochrome b_6f.[21−24] Structures of mitochondrial[6−19,25] and bacterial[20] Complex III, also known as cytochrome bc_1, have been

* To whom correspondence should be addressed.
† Current address: Division of Biological Chemistry and Molecular Microbiology, School of Life Sciences, University of Dundee, Dow St., Dundee DD1 5EH, U.K.; Tel: +7 (0)1382 348354.

(1) Walker, F. A.; Reis, D.; Balke, V. L. *J. Am. Chem. Soc.* **1984,** *106*, 6888−6898.
(2) Walker, F. A.; Huynh, B. H.; Scheidt, W. R.; Osvath, S. R. *J. Am. Chem. Soc.* **1986**, *108*, 5288−5297.
(3) Walker, F. A. *Chem. Rev.* **2004**, *104*, 589−615.
(4) Yatsunyk, L. A.; Carducci, M. D.; Walker, F. A. *J. Am. Chem. Soc.* **2003,** *125*, 15986−16005.
(5) Sun, F.; Huo, X.; Zhai, Y.; Wang, A.; Xu, J.; Su, D.; Bartiam, M.; Rao, Z. *Cell* **2005**, *121*, 1043−1067.
(6) Xia, D.; Yu, C.-A.; Kim, H.; Xia, J.-Z.; Kachurin, A. M.; Zhang, L.; Yu, L.; Deisenhofer, J. *Science* **1997**, *277*, 60−66.
(7) Iwata, S.; Lee, J. W.; Okada, K.; Lee, J. K.; Iwata, M.; Rasmussen, B.; Link, T. A.; Ramaswamy, S.; Jap, B. K. *Science* **1998**, *281*, 64−71.
(8) Zhang, Z.; Huang, L.; Shulmeister, V. M.; Chi, Y.-I.; Kim K. K.; Hung, L.-W.; Crofts, A. R.; Berry, E. A.; Kim, S.-H. *Nature* **1998**, *392*, 677−684.
(9) Berry, E. A.; Huang, L.-S.; Zhang, Z.; Kim, S.-H. *J. Bioenerg. Biomem.* **1999**, *31*, 177−190.
(10) Yu, C.-A.; Tian, H.; Zhang, L.; Deng, K.-P.; Shenoy, S. K.; Yu, L.; Xia, D.; Kim, H.; Deisenhofer, J. *J. Bioenerg. Biomem.* **1999**, *31*, 191−199.
(11) Berry, E. A.; Guergova-Kuras, M.; Huang, L.; Crofts A. R. *Annu. Rev. Biochem.* **2000**, *69*, 1005−1075.
(12) Gao, X.; Wen, X.; Yu, C.; Esser, L.; Tsao, S.; Quinn, B.; Zhang, L.; Yu, L.; Xia, D. *Biochemistry* **2002**, *41*, 11692−11702.
(13) Gao, X.; Wen, X.; Esser, L.; Quinn, B.; Yu, L.; Yu, C.-A.; Xia, D. *Biochemistry* **2003**, *42*, 9067−9080.
(14) Huang, L.; Cobessi, D.; Tung, E. Y.; Berry, E. A. *J. Mol. Biol.* **2005**, *351*, 573−597.

10.1021/ic060283h CCC: $33.50
Published on Web 06/16/2006

reported, and the resolution of the most recent structures is sufficient to reveal the geometry and the approximate histidine imidazole plane dihedral angles of the cytochrome *b* hemes to reasonably high accuracy. At present, imidazole dihedral angles of 86° and 64° are being used to model the low- and high-potential heme b_L and b_H centers, respectively, of the highest resolution (2.1Å)[25] bovine cytochrome bc_1 complex structure; the yeast structure, with the highest resolution 2.3 Å,[9,17] has those same angles as 84° and 71°. Among 10 recent structures from bovine, avian, yeast, and bacterial bc_1 complexes, the average angles are 84° ± 4° and 60° ± 7° for hemes b_L and b_H, respectively.[8,9,12−14,16,17,19,20,25] Much earlier, membrane-bound preparations of the cytochrome bc_1 complex were investigated in frozen solution by EPR spectroscopy, and the two *b* hemes were found to have single-feature EPR signals for heme b_L at $g = 3.75-3.78$[26−29] and for heme b_H at $g = 3.41-3.44$,[26−28] and between 3.49 and 3.60 for the yeast complex.[29]

The EPR spectra of model heme complexes, such as iron(III) tetraphenylporphyrins, $TPPFe^{III}$, with various axial ligands, were reported in the early 1980s as a function of solvent, ligand type, ligand basicity, porphyrin substituents, and mixed axial ligand coordination.[1,2] A major attempt was made to find correlations between the presumed orientation of the axial ligands and the EPR spectral type in order to use EPR parameters to predict molecular structures of heme centers in natural heme-containing systems. As a result of these efforts, the single-feature "large g_{max}" EPR signal was correlated with perpendicular ligand plane orientation and normal rhombic EPR signals with parallel.[2,30,31] However, this correlation was blurred by later studies where [(OETPP)Fe(4-Me_2NPy)$_2$]Cl, with $\Delta\varphi = 70°$, had a large g_{max} EPR signal,[32] while *paral*-[(TMP)Fe(5-MeHIm)$_2$]ClO_4, with $\Delta\varphi = 26°$ and 30° for two molecules in the unit cell,[35] had a normal rhombic EPR spectrum.[36] Finding low-spin ferriheme models with $\Delta\varphi$ between 30° and 70° has been of great interest for determining the angle at which the EPR spectral type changes from normal rhombic to large g_{max}.[3,4] The [(TPP)Fe(HIm)$_2$]Cl structure with $\Delta\varphi = 57°$ reported by Hoard in 1971[33] falls near the middle of the 30−70° range. The porphyrin core adopts a ruffled geometry with an average deviation of the meso carbons of ±0.32 Å and relatively short average Fe−N_P bonds of 1.989(5) Å.[33] Unfortunately, no EPR spectra were obtained for this sample, and all attempts to reproduce the crystals of Hoard have resulted in no crystals or crystals of different stoichiometry, unit cell, and/or low-spin ferriheme geometry.[31] Therefore, it was not possible to clearly assign the 57° angle as "parallel" or "perpendicular" on the basis of EPR spectral type. Knowing the angle at which the transition between the normal rhombic and large g_{max} EPR spectral types occurs would help in relating the EPR spectra of the membrane-bound cytochromes *b* of mitochondrial Complexes II and III and of chloroplast cytochrome b_6f to the intimate structures of the heme centers of these proteins.

In search of a bis-histidine-coordinated model system with intermediate angle between its axial ligands, we have crystallized many porphyrin complexes that show extreme flexibility of their porphyrin cores and wide ranges of axial ligand orientations. It was found for octamethyltetraphenylporphyrinatoiron(III) bis-ligated with *N*-methylimidazole, [(OMTPP)Fe(N-MeIm)$_2$]Cl, 4-dimethylaminopyridine, [(OMTPP)Fe(4-Me_2NPy)$_2$]Cl, 2-methylimidazole, [(OMTPP)Fe(2-MeHIm)$_2$]Cl, and for octaethyltetraphenylporphyrinatoiron(III) bis-ligated with 4-cyanopyridine, [(OETPP)Fe(4-CNPy)$_2$]ClO_4, that molecular structures, space group, porphyrin geometry, axial ligand orientation, and other parameters depend strongly on crystallization conditions.[4,34] For example, different forms of [(OMTPP)Fe(N-MeIm)$_2$]Cl with nearly parallel (19.5°) and exactly perpendicular (90°) ligand plane dihedral angles resulted from two crystallization trials, from methylene chloride-d_2/dodecane and chloroform/cyclohexane, respectively.[4] The same is true for bis-5-methylimidazole tetramesitylporphyrinatoiron(III), [(TMP)Fe(5-MeHIm)$_2$]ClO_4, where two structures with "parallel" (26° and 30°)[35] and "perpendicular" (76°) axial ligand arrangement have been reported.[36] The two crystalline forms each of [(OMTPP)Fe(N-MeIm)$_2$]Cl and [(TMP)Fe(5-MeHIm)$_2$]ClO_4 have distinctly different Mössbauer and EPR spectra.[4,36,37] On the other hand, [(OMTPP)Fe(4-Me_2NPy)$_2$]-

(15) Crofts, A. R. *Annu. Rev. Physiol.* **2004**, *66*, 689−733.
(16) Hunte, C.; Koepke, J.; Lange, C.; Rossmanith, T.; Michel, H. *Structure* **2000**, *8*, 669−684.
(17) Lange, C.; Nett, J. H.; Trumpower, B. L.; Hunte, C. *EMBO J.* **2001**, *20*, 6591−6600.
(18) Lange, C.; Hunte, C. *Proc. Natl. Acad. Sci. U.S.A.* **2002**, *99*, 2800−2805.
(19) Palsdottir, H.; Lojero, C. G.; Trumpower, B. L.; Hunte, C. *J. Biol. Chem.* **2003**, *278*, 31303−31311.
(20) Berry, E. A.; Huang, L.-S.; Saechao, L. K.; Pon, N. G.; Valkova-Valchanova, M.; Daldal, F. *Photosynth. Res.* **2004**, *81*, 251−275.
(21) Stroebel, D.; Choquet, Y.; Popot, J.-L.; Picot, D. *Nature* **2003**, *426*, 413−418.
(22) Durisu, G.; Zhang, H.; Smith, J. L.; Cramer, W. A. *Science* **2003**, *302*, 1009−1014.
(23) Cramer, W. A.; Zhang, H.; Yan, J.; Kurisu, G.; Smith, J. L. *Biochemistry* **2004**, *43*, 5921−5929.
(24) Smith, J. L.; Zhang, H.; Yan, J.; Kurisu, G.; Cramer, W. A. *Curr. Opin. Struct. Biol.* **2004**, *14*, 432−439.
(25) Protein Data Bank filename 2A06, deposited June, 2005.
(26) Orme-Johnson, N. R.; Hansen, R. E.; Beinert, H. *Biochem. Biophys. Res. Commun.* **1971**, *45*, 871−878.
(27) Salerno, J. C. *J. Biol. Chem.* **1984**, *259*, 2331−2336.
(28) Schütz, M.; Schoepp-Cothenet, B.; Lojou, E.; Woodstra, M.; Lexa, D.; Tron, P.; Dolla, A.; Durand, M.-C.; Stetter, K. O.; Baymann, F. *Biochemistry* **2003**, *42*, 10800−10808.
(29) Tsai, A.-L.; Palmer, G. *Biochim. Biophys. Acta* **1982**, *681*, 484−495.
(30) Scheidt, W. R.; Kirner, J. F.; Hoard, J. L.; Reed, C. A. *J. Am. Chem. Soc.* **1987**, *109*, 1963−1968.
(31) Scheidt, W. R.; Osvath, S. R.; Lee, Y. J. *J. Am. Chem. Soc.* **1984**, *109*, 1958−1963.
(32) Ogura, H.; Yatsunyk, L.; Medforth, C. J.; Smith, K. M.; Barkigia, K. M.; Renner, M. W.; Melamed, D.; Walker, F. A. *J. Am. Chem. Soc.* **2001**, *123*, 6564−6578.
(33) Collins, D. M.; Countryman, R.; Hoard, J. L. *J. Am. Chem. Soc.* **1972**, *94*, 2066−2072.
(34) Yatsunyk, L. A.; Walker, F. A. *Inorg. Chem.* **2004**, *43*, 757−777.
(35) Two molecules are found in the unit cell, one with an axial ligand plane dihedral angle of 26° and the other of 30°, but the two have similar angles, φ, from the N−Fe−N axes.[36] Although there is evidence of two overlapping EPR spectra, it was not possible to deconvolute the two because of the similarity of the *g* values.[36]
(36) Munro, O. Q.; Serth-Guzzo, J. A.; Turowska-Tyrk, I.; Mohanrao, K.; Shokhireva, T. Kh.; Walker, F. A.; Debrunner, P. G.; Scheidt, W. R. *J. Am. Chem. Soc.* **1999**, *121*, 11144−11155.
(37) Teschner, T.; Yatsunyk, L. A.; Schünemann, V.; Paulsen, H.; Winkler, H.; Hu, C.; Scheidt, W. R.; Walker, F. A.; Trautwein, A. X. *J. Am. Chem. Soc.* **2006**, *128*, 1379−1389.

Cl was crystallized in two forms with similar axial ligand orientation (close to perpendicular) but with strikingly different core geometry, almost purely saddled and saddled with ~30% ruffling (as judged by normal-coordinate structural decomposition, NSD, coefficients)[38] from chloroform/cyclohexane and methylene chloride/dodecane, respectively.[4] Two forms of crystals have been obtained for [(OETPP)Fe(N-MeIm)$_2$]Cl. We have previously reported the structure that resulted from the large dark-purple blocks crystallized from chloroform-*d*/cyclohexane. It revealed a highly nonplanar, purely saddled porphyrin core with axial ligand plane dihedral angle, $\Delta\varphi$, of 73.1°, and the average deviations of the β and meso carbons from the mean porphyrin plane of $\pm$1.24 and $\pm$0.03 Å, respectively.[4] The complex is characterized by a single-feature large g_{max}[1] or Type I[39] EPR signal with $g = 3.27$.[4] The second crystal form of [(OETPP)Fe(N-MeIm)$_2$]Cl was obtained from the same solvent system over a shorter period of time and with lower porphyrin concentrations. These crystals gave rise to a very different EPR spectrum with a mixture of rhombic and large g_{max} ($g \approx 3.0-3.3$) components that predicted both near-parallel and perpendicular ligand orientation on the basis of correlation of EPR spectral type with axial ligand orientation.[2-4]

In this paper, we present the crystal structure of this second set of [(OETPP)Fe(N-MeIm)$_2$]Cl crystals, together with the structures of [(OETPP)Fe(N-BzIm)$_2$]Cl and [(OETPP)Fe(HIm)$_2$]Cl, all of which crystallize in the same or related space groups and are characterized by a wide range of dihedral angles between the axial ligand planes, 16°, 30°, 45°, 56.8°, 57.2°, 59.6°, and 88.1°, all but the two extremes of which are intermediate between parallel and perpendicular orientations. The goal of the present studies of models of the cytochromes is to narrow the range of angles over which the type of EPR signal must switch from normal rhombic to large g_{max} and also to introduce a clearer view of what "perpendicular" and "parallel" actually mean in terms of EPR spectral type and its correlation with ligand orientation in the structures of bis-histidine-coordinated cytochromes of mitochondrial Complexes II and III.

Experimental Section

Materials. (OETPP)FeCl was prepared as reported previously.[4] Samples of [(OETPP)Fe(L)$_2$]Cl with L = HIm, N-BzIm, N-MeIm, and 4-MeHIm were prepared by addition of 3−6 equiv of axial ligand to purified (OETPP)FeCl in methylene chloride or chloroform solvent.[4]

EPR Spectra. EPR spectra of frozen solutions in CD_2Cl_2 and THF and finely ground crystalline samples of [(OETPP)Fe(HIm)$_2$]Cl, [(OETPP)Fe(N-BzIm)$_2$]Cl, [(OETPP)Fe(N-MeIm)$_2$]Cl, and [(OETPP)Fe(4-MeHIm)$_2$]Cl were recorded on a Bruker ESP-300E spectrometer (operating at 9.4 GHz with 0.2 mW microwave power, 100 kHz field modulation, and 1 G modulation amplitude) equipped with an Oxford Instruments ESR 900 continuous flow helium cryostat at 4.2 K.

X-ray Crystallography. Diffraction-quality crystals of [(OETPP)Fe(HIm)$_2$]Cl and [(OETPP)Fe(N-BzIm)$_2$]Cl were grown by the liquid diffusion method from a methylene chloride solution of the iron(III) porphyrinate complexes carefully layered with dodecane in NMR- or EPR-sized glass tubes over the course of 3−5 days. The same types of crystals were obtained from chloroform/cyclohexane. [(OETPP)Fe(N-MeIm)$_2$]Cl crystals of this report were grown via the diffusion of cyclohexane into the chloroform solution in 1−3 days. Crystallization of [(OETPP)Fe(N-MeIm)$_2$]Cl from methylene chloride/dodecane resulted in crystals of the same morphology and unit cell. All three sets of crystals were dark purple, small-sized parallelepipeds that decomposed easily at room temperature but were stable at 170 K or below over extended periods of time. In the case of [(OETPP)Fe(N-MeIm)$_2$]Cl, large blocks can be obtained while crystallizing from chloroform/cyclohexane in larger quantities (on the order of 50 mg) and over longer periods of time (on the order of 1 week). The structure of this crystalline form has been reported elsewhere.[4] Crystals of [(OETPP)Fe(4-MeHIm)$_2$]Cl were obtained from both THF and methylene chloride and used for EPR spectroscopy, but in both cases, they were of nondiffraction quality.

The paraton oil-coated crystals of each complex were mounted on glass fibers in random orientation and examined using Mo Kα radiation ($\lambda = 0.71073$ Å) on a Brucker SMART 1000 CCD area detector X-ray diffractometer at 100(2) K for [(OETPP)Fe(N-MeIm)$_2$]Cl and at 170(2) K for [(OETPP)Fe(HIm)$_2$]Cl and [(OETPP)Fe(N-BzIm)$_2$]Cl. Final cell constants and complete details of the intensity collection and least squares refinement parameters for all complexes are summarized in Table 1. Data were integrated using the Bruker SAINT software package's narrow frame algorithm[40] and corrected for absorption using SADABS.[41] All structures were solved by direct methods and refined by full-matrix least squares on F^2 values using the programs found in the SHELXTL (Version 6.12) suite.[42] Hydrogen atoms were added at idealized positions, constrained to ride on the atom to which they are bonded, and given thermal parameters equal to 1.2 or 1.5 times U_{iso} of that bonded atom.

The molecules of the porphyrinate complexes in all three structures form an open framework with large channels that can accommodate axial ligands of various sizes. All crystals were observed to break down rapidly on removal from the mother liquor, indicating the incorporation of a substantial amount of solvent in the lattice. The stability of crystals was greatly increased upon lowering the X-ray data collection temperature to at least 170 K, and the observed decay did not exceed 0.04%. It was possible to identify what appeared to be solvent molecules within the channels from difference Fourier syntheses; however, in all three cases, these could not be refined with reasonable structural parameters. Instead, the residual electron density due to solvent was treated using the method of Van der Sluis and Spek.[43] This gave the residual electron density and void volume corresponding to 5 molecules of CH_2Cl_2 per porphyrin complex for [(OETPP)Fe(HIm)$_2$]Cl, 4 molecules of $CHCl_3$ per porphyrin in [(OETPP)Fe(N-MeIm)$_2$]Cl, and 3 molecules of CH_2Cl_2 per porphyrin in [(OETPP)Fe(N-BzIm)$_2$]Cl. While not part of the atom list, the solvent molecules are included in the formulas, *F*000, density, and absorption coefficients. There is substantial disorder in each structure which was accounted for by the models used in each case (discussed below and in the Supporting

(38) Sun, L.; Jentzen, W.; Shelnutt, J. A. *The Normal Coordinate Structural Decomposition Engine*; http://jasheln.unm.edu/jasheln/content/nsd/NSDengine/.
(39) Walker, F. A. *Coord. Chem. Rev.* **1999**, *185−186*, 471−534.
(40) *Bruker 2002 SAINT Reference Manual Version 6.0*; Bruker AXS, Inc.: Madison, WI, 2002.
(41) Sheldrick, G. *SADABS 2.3*; University of Göttingen: Göttingen, Germany, 2002.
(42) *Bruker 2001 SHELXTL Reference Manual Version 6.12*; Bruker AXS, Inc.: Madison, WI, 2001.
(43) Van der Sluis, P.; Spek, A. L. *Acta Crystallogr.* **1990**, *A46*, 194−201.

Table 1. Summary of Crystal Data and Intensity Collection Parameters

molecule	[(OETPP)Fe(HIm)$_2$]Cl·5CH$_2$Cl$_2$	[(OETPP)Fe(N-BzIm)$_2$]Cl·3CH$_2$Cl$_2$	[(OETPP)Fe(N-MeIm)$_2$]Cl·4CHCl$_3$	[(OETPP)Fe(N-MeIm)$_2$]Cl·4CHCl$_3$ powder
empirical formula	$C_{71}H_{78}Cl_{11}FeN_8$	$C_{83}H_{86}Cl_7FeN_8$	$C_{72}H_{76}Cl_{13}FeN_8$	$C_{72}H_{76}Cl_{13}FeN_8$
fw	1489.21	1499.60	1570.11	1570.11
temp, K	170(2)	170(2)	100(2)	298
cryst syst	trigonal	trigonal	trigonal	trigonal
space group	$P3_221$	$P3_221$	$P3_1$	$P3_1$
a, b, Å	21.7714(11)	21.7519(8)	21.7611(3)	22.32(2)
c, Å	27.6277(18)	13.9290(10)	13.8520(4)	13.34(2)
α, β, γ, deg	90, 90, 120	90, 90, 120	90, 90, 120	90, 90, 120
V, Å^3	11340.9(11)	5707.5(5)	5680.7(2)	5756.4
Z	6	3	3	3
density (calcd), g/cm^3	1.308	1.309	1.377	
absorption coeff, mm^{-1}	0.633	0.494	0.704	
F(000)	4638	2355	2433	
cryst dimens, mm^3	0.34 × 0.27 × 0.22	0.42 × 0.17 × 0.13	0.41 × 0.19 × 0.10	
θ limits, deg	1.08−23.30	1.08−23.30	2.16−23.24	5.005−49.992
limiting indices	$-24 \le h, k \le 24$ $-30 \le l \le 30$	$-24 \le h, k \le 24$ $-15 \le l \le 15$	$-23 \le h, k \le 24$ $-15 \le l \le 15$	
flack param	0.08(3)	0.12(4)	0.09(3)	
reflns utilized	99 450	61 322	50 774	37
independ reflns [R_{int}, R_σ]	10 891 [0.1320, 0.084]	5498 [0.1753, 0.070]	10 852 [0.0649, 0.069]	
redundancy	9.13	11.2	4.7	
refln with $I > 2\sigma(I)$	7226 (66.3%)	4698 (85.0%)	7815 (72.0%)	
completeness, %	99.8	99.7	99.9	
min/max transmission	0.759278	0.925048	0.871758	
data/restraints/params	10 891/293/698	5498/420/485	10 852/1275/1012	
GOF on F^2	1.005	1.094	1.029	
final R indices [$I > 2\sigma(I)$]	R1 = 0.0791, wR2 = 0.2070	R1 = 0.0962, wR2 = 0.2344	R1 = 0.0779, wR2 = 0.2078	
R indices (all data)	R1 = 0.1067, wR2 = 0.2237	R1 = 0.1086, wR2 = 0.2433	R1 = 0.0968, wR2 = 0.2219	
largest diff. peak and hole, e/Å^3	0.418 and −0.382	0.439 and −0.336	0.487 and −0.541	
RMS diff. density, e/Å^3	0.064	0.078	0.059	

Information). This resulted in data-to-parameter ratios of 15.6, 11.3, and 10.7 for the HIm, N-BzIm, and N-MeIm complex structures, respectively, and data to (parameters + restraints) ratios of 11.0, 6.1, and 4.7, respectively.

[(OETPP)Fe(N-BzIm)$_2$]Cl. The asymmetric unit contains one porphyrin molecule that occupies a 2-fold axis, with the benzyl imidazole ligands disordered about the axis. The phenyl group of the N-BzIm ligand A could be distinguished without difficulty. The phenyl group of ligand B could not be so well distinguished; the atoms of the phenyl ring that could be identified from difference Fourier synthesis were used as the base atoms for a fitted hexagon group. The hexagon constraint and common isotropic thermal parameter (refined via a free variable) were used throughout the refinement of both benzyl groups. Each pendant phenyl group on the porphyrin core was disordered over two close-in-space positions with half-occupancy. Distance restraints were applied to the C−C bond lengths, and similarity and rigid bond restraints were used in the refinement of the anisotropic thermal parameters. The chloride anion that sits on a general position was fixed at half-occupancy for charge balance. Its poor thermal parameters are likely to be a result of anion disorder within the channel. Additional details concerning the structure solution of this and other complexes under study are included in the Supporting Information.

[(OETPP)Fe(HIm)$_2$]Cl. The asymmetric unit contains two crystallographically inequivalent half porphyrin molecules (**1** and **2**) each on a 2-fold axis, with HIm ligands disordered about this axis. The chloride anion is disordered over two positions, each with half-occupancy. The unit cell is doubled in c with respect to the *N*-methylimidazole and *N*-benzylimidazole crystal structures (Table 1). It is possible to index the diffraction pattern with a unit cell where $c = 13.788$ Å; however, this cell leaves a significant number of spots with $l = 0.5$ from integer values (Figure S1). The MISSYM algorithm in Platon[44] was used to check for missed translational symmetry in the structure, but none was found.

[(OETPP)Fe(N-MeIm)$_2$]Cl. The first of these three crystal structures to be solved was that of [(OETPP)Fe(N-MeIm)$_2$]Cl, and from the first tentative solution, there was a question as to whether the crystals might be merohedral twins, especially because of the large apparent void space that was, at that first solution, believed to have only one chloroform molecule per iron porphyrin complex unit. A number of tests were made at that time (2001) and since to verify whether the crystals were merohedral twins. For that complex, two space groups were considered, $P3_121$ and $P3_1$, the latter of which yielded better R indices and RMS difference density. Diffraction spot shapes were also scrutinized carefully for signs of asymmetry; none was found. Then, the powder diffraction data discussed below was obtained to see if the unit cell was the same as found by single-crystal techniques, which it was. Finally, a fresh model was created from the raw data. WinGX[45] was used to evaluate putative values of R(sym) in all Laue classes from the raw, uncorrected data. For [(OETPP)Fe(N-MeIm)$_2$]Cl it reported 0.072 for Laue class −3 but 0.121 for −3m. Increasing the space group symmetry from $P3_1$ to $P3_121$ effectively adds a 2-fold rotation axis through the iron center and perpendicular to the porphyrin ring, with the iron located on the rotation axis. While the porphyrin core is compatible with this symmetry element (as evidenced by the data sets for the other two complexes) the axial ligands are not. The ligands suffer from both substitutional (exchanging places of the N and C atoms) and static/positional disorder. This second disorder is incompatible with the 2-fold axis, and the ligands could not be refined anisotropically. It is thus proposed that this rotation is a *pseudo*-symmetry element only, rather than a genuine symmetry element as found in the other two complexes (which are compatible with the 2-fold rotation, since the axial ligands do not suffer from the same disorder). This is supported by the ADDSYM-EXT routine in PLATON,[44] which does not detect missed symmetry in space group $P3_1$. For these reasons, we are convinced that $P3_1$ is the correct space group for this complex.

(44) Spek, A. L. *J. Appl. Crystallogr.* **2003**, *36*, 7−13.
(45) Farriguia, L. J. *J. Appl. Crystallogr*. **1999**, *32*, 837−838.

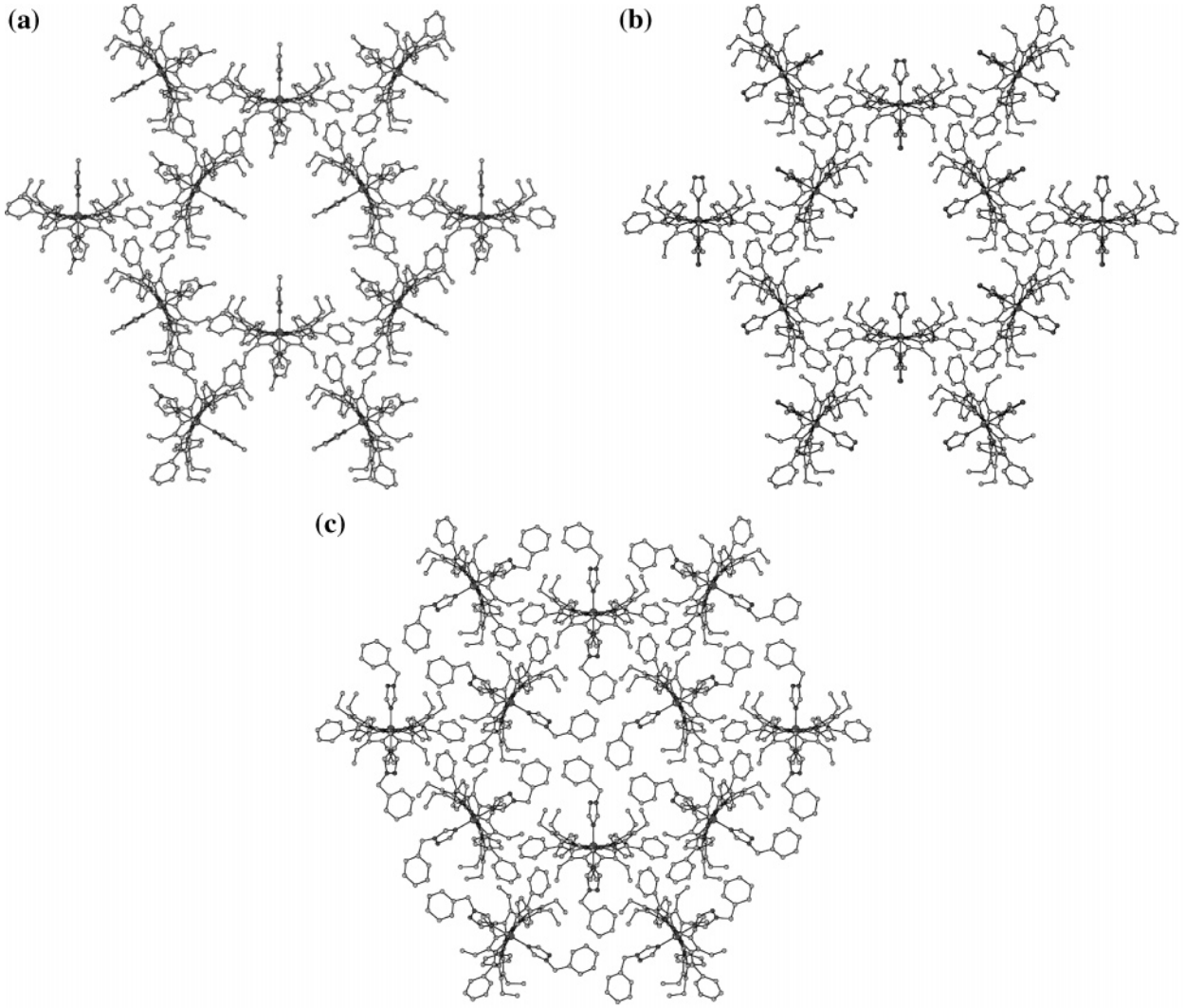

Figure 1. Packing diagrams, showing two types of channels in (a) [(OETPP)Fe(N-MeIm)$_2$]Cl, (b) [(OETPP)Fe(HIm)$_2$]Cl, and (c) [(OETPP)Fe(N-BzIm)$_2$]-Cl. Large channels are occupied with imidazole axial ligands, and small channels are occupied with pendant phenyl groups of the porphyrin. In each case, three imidazole groups penetrate further into the large channels than the other three. The size of the large void is such that ligands of various sizes fit in without change in lattice dimensions.

There is one crystallographically independent molecule on a general position in this structure. For this reason, the space group $P3_1$ was chosen over $P3_121$. Similarity restraints corresponding to a 2-fold axis were used in refinement of the porphyrin core. On one side of the porphyrin core, the axial ligand is disordered over two positions (A and C) with 0.584(12) occupancy of A and a 28.6(10)° angle between A and C; on the other side, it is disordered over two positions (B and D) with 0.772(10) occupancy of B and a 43.5(11)° angle between B and D. The axial ligands were refined using restrained anisotropic thermal parameters, similarity and rigid bond restraints, and flat geometry. Distance restraints based on the geometry of other imidazole ligands in the Cambridge Structural Database were used. The disorder of pendant phenyl rings on the porphyrin core was modeled in the same way as for the [(OETPP)-Fe(N-BzIm)$_2$]Cl complex.

Powder Diffraction of [(OETPP)Fe(N-MeIm)$_2$]Cl. As a check for polymorphic crystal forms and to confirm the single-crystal unit cell parameters for [(OETPP)Fe(N-MeIm)$_2$]Cl, the diffraction pattern for a polycrystalline sample maintained in solvent was acquired. Crushed crystals and a small amount of mother liquor were pipeted into a 0.5 mm glass capillary tube which was mounted and spun on a PANAlytical XPert MPD powder diffractometer. All measurements utilized Cu Kα radiation (λ = 1.5418Å). An incident beam parabolic X-ray mirror was used to produce parallel beam conditions. The detector used was a PANAlytical X'Celerator, a solid-state RTMS array covering ~2° 2θ with 112 channels. The scan range was 5−50° 2θ, the step size was ~0.017°, and the scan time was 1 h, which equates to a counting time of 180 s/step. Thirty-seven observed peaks were fit to the expected unit cell parameters using the PANAlytical X'Pert Plus refinement software package. Results are summarized in Table 1.

Results and Discussion

Crystal Structures of the Iron(III) Porphyrinate Ions. The crystal structures of bis-ligated (OETPP)Fe^{III} with HIm, N-MeIm, and N-BzIm all have the same basic structural motif, which consists of stacks of porphyrin molecules aligned parallel to the plane of the porphyrin core. A 3-fold screw axis links these stacks into a three-dimensional framework; the resulting structure contains large channels filled with disordered solvent molecules and one each of the axial imidazole ligands (Figure 1a−c). Six porphyrin molecules in total form the sides of one channel. The ligands

on either side of the porphyrin molecule penetrate the channel differently; three imidazole groups penetrate further into the channel than the other three. There is a second smaller void filled with pendant phenyl rings from the porphyrin core (Figure 1a−c) that results in high phenyl ring disorder (see Experimental Section). The existence of the large voids and the spatial orientation of the porphyrin molecules in the crystal structure of (OETPP)Fe^{III} with different imidazole ligands makes the basic motif very flexible; it can accommodate ligands as large as N-BzIm and as small as HIm without significant change in cell dimensions but with different amounts of disordered solvent; the amount of disordered solvent is inversely related to the size of the ligand, with five solvent molecules for the HIm complex, four for the N-MeIm complex, and three for the N-BzIm complex.

The respective unit cell length for all three crystal structures of this work is very similar (Table 1). The deviation of the powder diffraction data for [(OETPP)Fe(N-MeIm)$_2$]-Cl is probably due to the difference in the temperature of the measurement and possible difference in solvent content of the crystallites. The overall similarity in cell parameters and the identity of the space group for the powder diffraction measurements on [(OETPP)Fe(N-MeIm)$_2$]$^+$ confirm the assignment of the space group for this, and by analogy, the bis-HIm and bis-N-BzIm complexes. The doubling in *c* for the imidazole structure may be artificial; a full description of the reasons for this cell choice is given in the Supporting Information. The doubling in *c* results in two independent half-molecules of [(OETPP)Fe(HIm)$_2$]Cl in the asymmetric unit. Their conformations are similar, with slight difference in the position of the ethyl and phenyl groups (Supporting Information, Figure S2) and a primary difference in the orientation of the axial ligands. Similarly, the change in point group from $-3m1$ to -3 for the N-MeIm structure is due to different disorder of the axial ligands rather than any major difference in overall crystal structure. Since the chirality of the structure results from the three-dimensional arrangement of achiral molecules, no significance is attached to the presence of a 3_1 rather than 3_2 axis; different crystals may have different hands.

The molecular structure of [(OETPP)Fe(N-MeIm)$_2$]Cl, shown as ORTEP diagrams in two views, is presented in Figure 2, together with the numbering scheme for the crystallographically unique atoms. The porphyrin core in this and other structures of the present study clearly adopts a saddled geometry with the average deviation of the pyrrole β carbons of $\pm$1.13, 1.14, 1.15, and 1.15 Å for (OETPP)-Fe^{III} with HIm (**1** and **2**), N-BzIm, and N-MeIm, respectively. Thermal ellipsoid plots for the other two complexes are shown in Supporting Information Figures S3 and S4, where it can be seen that because of the higher temperature of those structure determinations (170° as compared to 100°) the thermal ellipsoids are larger. The saddled geometry of the porphyrin core is obvious from Figure 3 and from the results of the NSD method (Table 2).[38] The NSD method describes each porphyrin in terms of displacement along the lowest-frequency normal coordinates that correspond to one of the

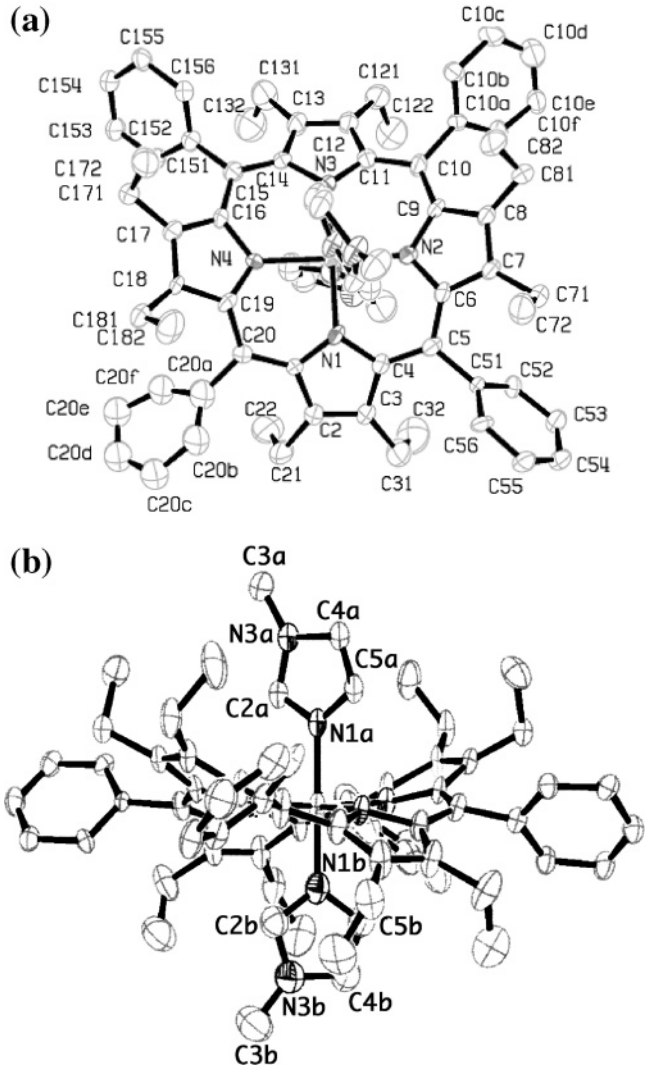

Figure 2. ORTEP plot of the porphyrin macrocycle of [(OETPP)Fe(N-MeIm)$_2$]Cl, with the numbering scheme for unique atoms: (a) top view; (b) side-on view. Thermal ellipsoids are shown at 50% probability, and H-atoms are omitted for clarity. Thermal ellipsoid plots for [(OETPP)Fe-(HIm)$_2$]Cl molecules 1 and 2 and [(OETPP)Fe(N-BzIm)$_2$]Cl are shown in Supporting Information Figures S3 and S4, respectively.

porphyrin distortion modes: B_{2u} (saddle), B_{1u} (ruffle), A_{2u} (dome), $E_g(x)$ (wave(x)), $E_g(y)$ (wave(y)), and A_{1u} (propeller). Each porphyrin under study is characterized by a large and similar B_{2u} (saddle) coefficient of 3.4310, 3.4524, 3.4909, and 3.4698 for [(OETPP)Fe(HIm)$_2$]Cl (**1** and **2**), [(OETPP)-Fe(N-BzIm)$_2$]Cl, [(OETPP)Fe(N-MeIm)$_2$]Cl, respectively. All other coefficients are either small or negligible except B_{1u} (ruffle) in the case of [(OETPP)Fe(HIm)$_2$]Cl, **1** and **2**, which is equal to 0.5447 and 0.5229, respectively. In accord with these results, the deviations of the meso carbons from the mean porphyrin plane, $|\Delta C_m|$, are 0.20, 0.19, 0.02, and 0.01 Å for (OETPP)Fe^{III} with HIm (**1** and **2**), N-MeIm, and N-BzIm, respectively (Table 3). In short, both structures of [(OETPP)Fe(HIm)$_2$]Cl are saddled with some ruffling (~13%) while structures of [(OETPP)Fe(N-MeIm)$_2$]-Cl and [(OETPP)Fe(N-BzIm)$_2$]Cl are purely saddled. The previously reported structure of [(OETPP)Fe(N-MeIm)$_2$]Cl,[4] where $|\Delta C_\beta| = 1.24$ Å and $|\Delta C_m| = 0.03$ Å, is also purely saddled.

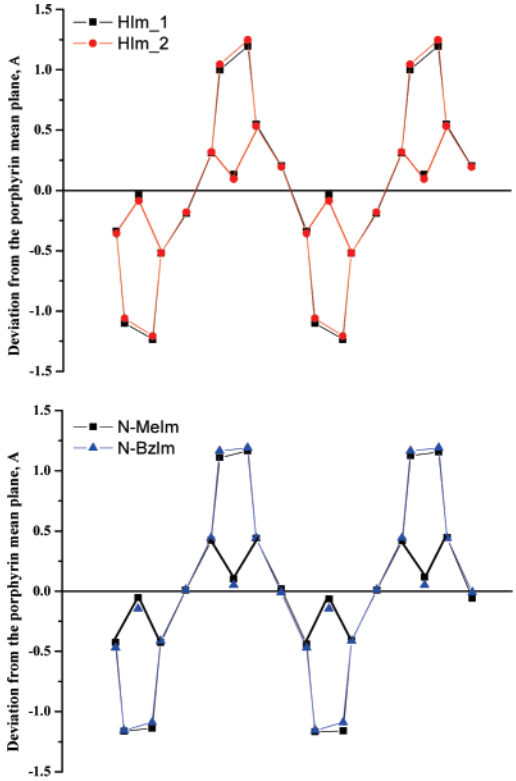

Figure 3. Linear representation of the deviation of the macrocycle atoms form the mean porphyrin plane.

The key feature of the current structure determinations of (OETPP)Fe^{III} with different imidazoles is the orientation of the axial ligands. The axial ligand plane dihedral angles, $\Delta\varphi$, range from 16.0 to 88.1°, with intermediate values of 30.1°, 44.6°, 56.8°, 57.2°, and 59.6°, most of which fall well between strictly parallel and perpendicular orientations. Such structures have been long awaited in the porphyrin field. There are two independent molecules in the crystal structure of [(OETPP)Fe(HIm)$_2$]$^+$Cl$^-$ which are characterized by substantially different $\Delta\varphi$ of 30.1(4)° and 57.2(6)°. Such a large (30°, as well as 26° for the second molecule in the unit cell)[35,36] "parallel" dihedral angle between the axial ligand planes was observed earlier for *paral*-[(TMP)Fe(5-MeHIm)$_2$]ClO$_4$, which has a single normal rhombic EPR spectrum.[36] On the other hand, the angle of 57.2° is unique and can be the largest "parallel" or the smallest "perpendicular" dihedral angle reported thus far. It is very similar to the 57° angle of Hoard's structure of [(TPP)Fe(HIm)$_2$]Cl,[33] the EPR spectrum of which was never recorded, as well as to the 56.8(5)° angle of the [(OETPP)Fe(N-BzIm)$_2$]Cl structure of this study, but as will be discussed below, the two have different EPR spectral types.

In the structure of [(OETPP)Fe(N-MeIm)$_2$]Cl, the axial N-MeIm ligand is disordered over two positions on both sides of the porphyrin core. The angles between the major and minor component of each ligand are 28.6(10)° and 43.5(11)°, for L1 and L2, respectively. Such a disorder results in the following distribution of molecules with $\Delta\varphi$ values of 16.0(6)° (32% of molecules), 44.6(5)° (45%), 59.6(11)° (10%), and 88.1(9)° (13%). Dihedral angles of 44.6° and 59.6° have never been observed previously for severely nonplanar saddled iron porphyrinate structures. The earlier-reported structure of [(OETPP)Fe(N-MeIm)$_2$]Cl,[4] crystallized from chloroform-*d*/cyclohexane, was characterized by a dihedral angle $\Delta\varphi = 73.1°$ between the axial ligand planes; these crystals exhibited a large g_{max} EPR signal, $g_{max} = 3.27$.

The imidazole ligands in the (OETPP)Fe^{III} structures are nearly perpendicular to the porphyrin core with the dihedral angle between the ligand plane and porphyrin mean plane ranging from 87.7° to 90.0° (Table 3). Similar results are obtained for the previously reported structure of [(OETPP)-Fe(N-MeIm)$_2$]Cl,[4] where the same angles are 86.7° and 87.5°, just slightly smaller than in the structures under study.

The projection of the plane of the axial ligands form angles $\varphi = 11.1°$ and 19.0° to the N$_p$−Fe−N$_p$ axis in the structure of [(OETPP)Fe(HIm)$_2$]Cl (**1**) and 12.1° and 17.2° angles in the structure of [(OETPP)Fe(HIm)$_2$]Cl (**2**), 27.6° and 18.0° angles in the structure of [(OETPP)Fe(N-MeIm)$_2$]Cl (for the major component of axial ligands), and 2.7° and 34.2° angles in the structure of [(OETPP)Fe(N-BzIm)$_2$]Cl. Most of these φ angles are far from the optimal value of 2−3° predicted from molecular mechanics calculations for severely nonplanar saddled structures of dodecasubstituted Co(III) porphyrin macrocycles with various axial imidazole ligands, [(OETPP)-Co(L)$_2$]$^+$ (where L is N-MeIm or N-PhIm).[46]

The average dihedral angles between the porphyrin mean plane and the phenyl rings are relatively small and similar to each other, 46.7(2)°, 46.1(2)°, 45.5(6)°, and 47.4(8)° for [(OETPP)Fe(HIm)$_2$]Cl (**1**, **2**), [(OETPP)Fe(N-MeIm)$_2$]Cl, and [(OETPP)Fe(N-BzIm)$_2$]Cl, respectively. Low values of the phenyl dihedral angles indicate a high degree of saddle distortion. Indeed, the planarity of the porphyrin core increases on going from OETPP to OMTPP and then to TC$_6$TPP (Δ24 = 0.59 > 0.54 > 0.48 = 0.48 > 0.30 Å), and so does the value of the phenyl dihedral angle (40.0° < 45.5° < 47.0° ≈ 46.3° < 71.8°) for [(OETPP)Fe(N-MeIm)$_2$]Cl ($\Delta\varphi$ = 73.1°),[4] [(OETPP)Fe(N-MeIm)$_2$]Cl ($\Delta\varphi = 44.6°$) (this work), [(OMTPP)Fe(N-MeIm)$_2$]Cl ($\Delta\varphi$ = 19.5°),[4] [(OMTPP)Fe-(N-MeIm)$_2$]Cl ($\Delta\varphi = 90°$),[4] and [(TC$_6$TPP)Fe(N-MeIm)$_2$]-Cl ($\Delta\varphi = 90°$).[4] The C−C$_{Ph}$ bond clearly stays single despite some conjugation between the porphyrin core and phenyl groups: 1.484(8), 1.506(8), 1.50(2), and 1.54(2) Å for OETPPFe^{III} with HIm (**1**, **2**), N-MeIm, and N-BzIm.

The average values for selected bond distances and angles with estimated standard deviation for all complexes under study are included in Figure 4 and Table 3. Fe−N$_p$ distances are 1.961−1.982 Å and are typical for low-spin (OETPP)-Fe^{III} complexes. The same is true for the Fe−N$_{ax}$ distances.

EPR Spectroscopy of the Crystalline Iron(III) Porphyrinates. Representative EPR spectra for complexes of (OETPP)Fe^{III} with two N-BzIm, 4-MeHIm, HIm, and N-MeIm are shown in Figure 5.

The crushed crystalline samples of [(OETPP)Fe-(HIm)$_2$]Cl obtained from both methylene chloride/dodecane and chloroform/cyclohexane solvent systems showed almost

(46) Medforth, C. J.; Muzzi, C. M.; Shea, K. M.; Smith, K. M.; Abraham, R. J.; Jia, S.; Shelnutt, J. A. *J. Chem. Soc., Perkin Trans. 2* **1997**, 833−837.

Table 2. Normal-Coordinate Structural Decomposition (NSD) of Distortion Modes of Complexes under Study

compound	D_{oop}	B_{2u}, saddle	B_{1u}, ruffle	A_{2u}, dome	$E_g(x)$, wave(x)	$E_g(y)$, wave(y)	A_{1u}, propeller	sum	ruf/sum, %
[(OETPP)Fe(HIm)$_2$]Cl, **1**	3.4770	3.4310	0.5447	0.1351	0.0006	0.0007	0.0584	4.1705	13.1
[(OETPP)Fe(HIm)$_2$]Cl, **2**	3.4924	3.4524	0.5229	0.0320	0.0004	0.0006	0.0538	4.0621	12.9
[(OETPP)Fe(N-MeIm)$_2$]Cl	3.4714	3.4698	0.0504	0.0652	0.0287	0.0285	0.0500	3.6926	1.4
[(OETPP)Fe(N-MeIm)$_2$]Cl[a]	3.7347	3.7320	0.0792	0.0360	0.1054	0.0315	0.0108	3.9949	2.0
[(OETPP)Fe(N−BzIm)$_2$]Cl	3.4943	3.4909	0.0560	0.1224	0.0009	0.0006	0.0780	3.7488	1.5

[a] Data taken from ref 4.

Table 3. Comparison of Structural Parameters for Complexes of This Study

complex	Fe−N_P Å	Fe−N_{ax} Å	angle φ between N−Fe−N axis and ligand planes, deg[d]	dihedral angle between axial ligand planes, $\Delta\varphi$, deg	av dihedral angle of phenyls, deg	tilt angle of axial ligand, deg	av $\lvert\Delta C_m\rvert$ Å	av $\lvert\Delta C_\beta\rvert$ Å	Δ_{24} Å[c]
[(OETPP)Fe(HIm)$_2$]Cl, **1**	1.980(4)	1.936(9) 1.998(7)	11.1(4); −19.0(2)	30.1(4)	46.7(2)	90.0(1)	±0.196	±1.133	0.580
[(OETPP)Fe(HIm)$_2$]Cl, **2**	1.961(4)	1.962(7) 1.973(9)	12.1(5) 72.3(5)	57.2(5)	46.1(2)	90.0(1)	±0.188	±1.140	0.585
[(OETPP)Fe(N-MeIm)$_2$]Cl	1.964(5)	1.996(5) 1.956(6)	27.6(7) 72.0(5)	44.6(5)[a]	45.5(6)	87.7(2) 89.7(2)	±0.023	±1.148	0.543
[(OETPP)Fe(N-MeIm)$_2$]Cl[b]	1.970(7)	1.976(3) 1.978(3)	9.6; 82.7	73.1	40.0	86.7 87.5	±0.030	±1.235	0.587
[(OETPP)Fe(N-BzIm)$_2$]Cl	1.982(5)	1.988(10) 1.992(8)	−2.2(7); 54.6(4)	56.8(5)	47.4(8)	90.0(2)	±0.011	±1.151	0.565

[a] Results are given only for the major component of the axial ligands. [b] Data taken from ref 4. [c] Δ24 is the average deviation of all core atoms from the mean porphyrin plane defined by four nitrogens. [d] The orientation with respect to the core is relative to the N(imidazole)−Fe−N(porphyrin) plane.

identical EPR spectra (Figure 5 for HIm complexes, red and black traces, respectively) with two types of signals: large g_{max} with slightly different g values (g = 3.24 and 3.17, respectively) and identical normal rhombic, with g = 2.76, 2.35, and 1.63, $\Sigma g^2 = 15.80$, with calculated crystal field parameters[47−50] $V/\lambda = 2.39$, $\Delta/\lambda = 2.96$, and $V/\Delta = 0.81$. The presence of two EPR signals, one of each type, is interesting in view of the fact that the structure shows two molecules, **1** and **2**, in the unit cell. The normal rhombic EPR signal must correspond to molecule **1** with $\Delta\varphi$ = 30.1(4)°. Similar normal rhombic EPR spectra were observed for *paral*-[(TMP)Fe(5-MeHIm)$_2$]ClO_4 with $\Delta\varphi$ = 26° and 30°.[35,36] Thus, the large g_{max} signal must correspond to molecule 2 with $\Delta\varphi$ = 57.2(6)°, which identifies this angle as the smallest "perpendicular" angle reported thus far. It should be noted that the amplitude of the derivative mode signal for the large g_{max} EPR type is small because the spectrum is spread over a considerably larger magnetic field range than the rhombic signal with g = 2.76, 2.35, 1.63 and because such signals tend to have short relaxation times. Intensities of the two signals can only be compared from the integral of the absorption mode spectra, the double integral of the derivative mode spectra actually recorded. Since the structure was solved for the chloroform/cyclohexane-derived crystals, the relevant large g_{max} value for the 57.2° angle is 3.24.

The ground crystalline sample of the *N*-benzylimidazole complex of (OETPP)Fe^{III} displays two rhombic signals in its EPR spectrum, a major signal, with g values of 3.08 and 2.19, Figure 5. Using $\Sigma g^2 = 16.00$, the third g value is calculated to be 1.31. This gives $V/\lambda = 1.49$, $\Delta/\lambda = 3.00$, and $V/\Delta = 0.5$. A minor signal was also observed, with g = 2.79, 2.34, and 1.58, $\Sigma g^2 = 15.76$, $V/\lambda = 2.24$, $\Delta/\lambda = 2.86$, and $V/\Delta = 0.78$. The nature of the species that gives rise to this minor signal is unknown; it may arise from the molecules in the mother liquor that accompanied the polycrystals to keep them from decomposing. The major rhombic signal is expected to be that of the single species observed in the crystal structure, which has the *N*-benzylimidazole planes with $\Delta\varphi$ = 56.8(5)°. Thus, on the basis of the rhombic EPR signal observed, this molecule has the largest "parallel" dihedral angle reported thus far. The major EPR signal of [(OETPP)Fe(N-BzIm)$_2$]Cl is very much like that of horse heart cytochrome *c* and bacterial cytochrome c_2, which have very similar g values (3.06, 2.25, 1.25 and 3.13, 2.11, 1.23, respectively) with a poorly resolved or unobservable third g value at the high-field position.[51,52]

The sample of [(OETPP)Fe(N-MeIm)$_2$]Cl has a large signal centered at g = 3.15 that extends from g = 3.0 to g = 3.3 that clearly consists of several overlapping features, plus peaks at 2.79 and 2.52, center derivative features at 2.35 and 2.20, and minimum g-value features at 1.81, 1.62, and 1.39. On the basis of the spectral simulation shown in Supporting Information Figure S5, these features are interpreted as two large g_{max} signals with $g \approx 3.3$ (13%) and 3.2 (10%), and four rhombic signals (g = 3.15, 2.19, 1.18, Σg^2 = 16.00, $\Delta/\lambda = 2.66$, $V/\lambda = 1.34$ (45%); g = 3.04, 2.20, 1.39, $\Sigma g^2 = 16.00$; $\Delta/\lambda = 3.22$, $V/\lambda = 1.60$ (32%); g = 2.79, 2.36, 1.62, Σg^2 = 16.00, $\Delta/\lambda = 2.92$, $V/\lambda = 2.33$ (10%); and g = 2.52, 2.31, 1.81, $\Sigma g^2 = 14.96$, $\Delta/\lambda = 3.59$, V/λ =

(47) Griffith, J. S. *Mol. Phys.* **1971**, *21*, 135−139.
(48) Blumberg, W. E.; Peisach, J. *Adv. Chem. Ser.* **1971**, *100*, 271−291.
(49) Peisach, J.; Blumberg, W. E.; Adler, A. D. *Ann. N. Y. Acad. Sci.* **1973**, *206*, 310−327.
(50) Taylor, C. P. S. *Biochim. Biophys. Acta* **1977**, *491*, 137−149.
(51) Trautwein, A. X.; Bill, E.; Bominaar, E. L.; Winkler, H. *Struct. Bonding* **1991**, *78*, 1−95.
(52) Huynh, B. H.; Emptage, M. H.; Münck, E. *Biochim. Biophys. Acta* **1978**, *534*, 295−306.

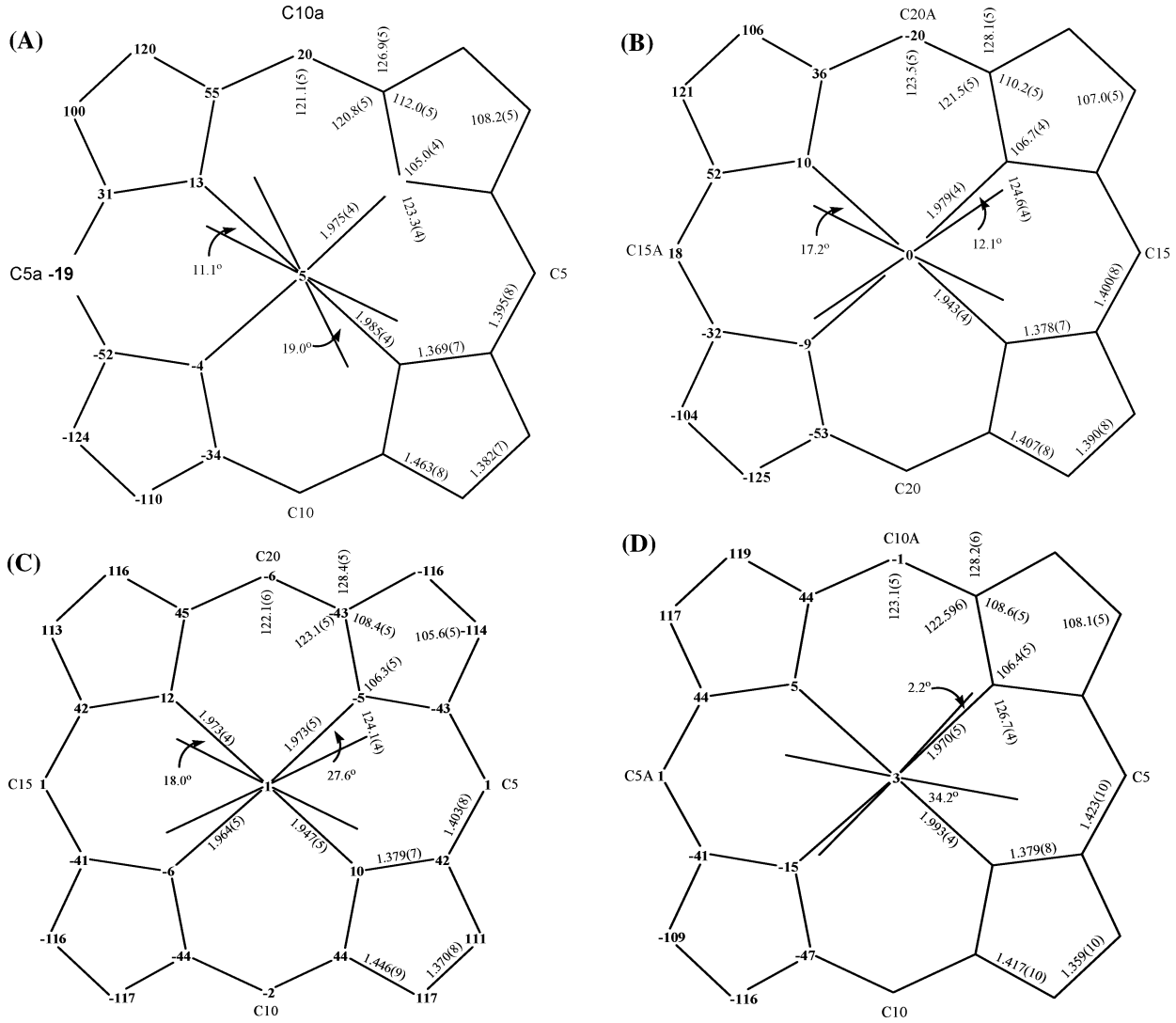

Figure 4. Formal diagram for (A) [(OETPP)Fe(HIm)$_2$]Cl, **1**; (B) [(OETPP)Fe(HIm)$_2$]Cl, **2**; (C) [(OETPP)Fe(N-MeIm)$_2$]Cl; and (D) [(OETPP)Fe(N-BzIm)$_2$]-Cl. Shown are the displacement of the atoms in units of 0.01 Å from the mean porphyrin plane of the 24-atom core of each molecule. The orientation of the axial ligands with the closest N_P-Fe-N_P vector and selected bond length and angles are also included into the diagram. For (C), only the orientations of the axial ligands of the major species are shown.

3.63 (2%)). The dihedral angles between the axial ligand planes observed for the crystals of [(OETPP)Fe(N-MeIm)$_2$]-Cl with disordered axial ligand orientations and their relative abundances are 16.0(6)° (32%), 44.6(5)° (45%)°, 59.6(11)° (10%), and 88.1(9)° (13%). Thus, the large g_{max} values are assigned to the molecules with 88.1° and 59.6° dihedral angles between their axial ligand planes ($g = 3.3$ and 3.2, respectively, consistent with the switch in spectral type at approximately 57°). The rhombic signals are assigned to the major species with $\Delta\varphi = 44.6°$ and 16.0° ($g_{max} = 3.14$ and 3.04, 45% and 32%, respectively). We do not know the source of the two low-intensity rhombic signals. The $g = 2.79$, 2.36, 1.62 signal is very similar to that observed for the N-BzIm complex. It is possible that this signal also arises from the molecules of the complex present in the mother liquor that accompanied the crushed crystals to maintain their stability. The last rhombic signal represents a species of very low abundance, ~2%, and we do not know its origin. Although the percentages given in the previous sentences add up to more than 100%, they should be viewed simply as scaling factors that relate the relative intensities of the various features to each other.

While the simulation of this spectrum shown in Supporting Information Figure S5 yields an acceptable explanation of the species that contribute to the observed spectrum (except for the broad background from about 3000 G to the end of the field sweep of the experimental spectrum, which is likely caused by molecular oxygen in the EPR tube), it is probably not a unique explanation of that spectrum. This, together with the disordered axial ligand plane orientations, makes this sample less useful than it might otherwise be. Thus, it is gratifying that the key axial ligand plane orientations and EPR signals are observed for the bis-N-BzIm and -HIm complexes of this study. The N-MeIm complex data simply help to show that there is no major break in the plot of g_{max} vs $\Delta\varphi$, shown in Figure 6.

Finally, the spectrum of a ground crystalline sample of [(OETPP)Fe(4-MeHIm)$_2$]Cl (from THF) consists of three sets of signals, large g_{max} with $g = 3.14$ and two-well resolved normal rhombic signals with $g = 2.82$, 2.36, and 1.58 and g

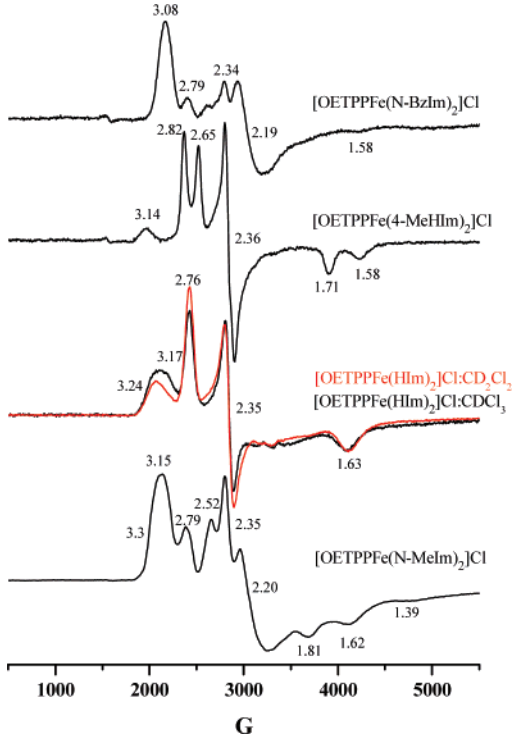

Figure 5. EPR spectra at 4.2 K of crystalline [(OETPP)Fe(L)$_2$]Cl with L = N-BzIm, 4-MeHIm, HIm, and N-MeIm. Fits of the N-MeIm spectrum are shown in Supporting Information Figure S5a and b.

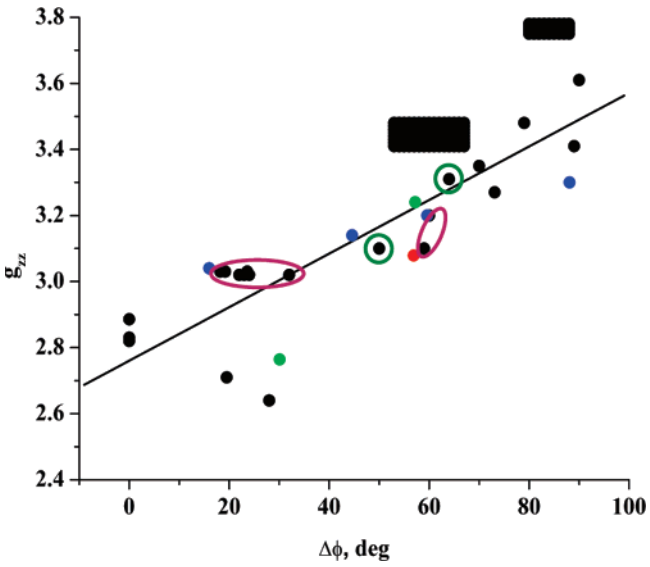

Figure 6. Correlation of the largest g value with the dihedral angle between axial ligand planes. Symbols: black, structures and g values reported previously;[2,4,32,36,53−57,59,60] red, *N*-benzylimidazole complex, 100% $\Delta\varphi$ = 56.8°; green, HIm complex, 50% $\Delta\varphi$ = 30.1°, 50% $\Delta\varphi$ = 57.2°; blue, *N*-methylimidazole complex, 32% 16.0°, 45% 44.6°, 10% 59.6°, 13% 88.1°. The two points represented as black rectangles, centered at 60° and 84°, represent the range of g values[26−28] and the average current histidine imidazole plane dihedral angles of the b_H and b_L hemes, respectively, of 10 recent structures of Complex III from a wide range of species,[8,9,12−14,16,17,19,20,25] with the deviations from the averages for each shown by the width and height of the two rectangles. Proteins other than Complex III cytochromes *b* are enclosed in ovals or circles, purple for water-soluble proteins and green for membrane-bound proteins.

= 2.65, 2.36, and 1.71. With these, we can predict at least two different orientations of the axial ligand planes: one set of molecules with "perpendicular" axial ligands and one or two sets of molecules with "parallel" axial ligand planes, depending on whether the second rhombic signal is from molecules in the crystals or in the mother liquor that accompanied them. Judging by the size of the largest g value for all three signals, g = 3.14, 2.82, and 2.65 and based upon the correlation between $\Delta\varphi$ and the largest g value discussed below, we can predict angles close to 60°, 30°, and 0°, respectively. A similar EPR spectrum is observed for the frozen solution of [(OETPP)Fe(4-MeHIm)$_2$]Cl in CD_2Cl_2, which shows two overlapping rhombic signals with g = 2.91, 2.27, 1.53 and g = 2.69, 2.43, 1.69. Unfortunately, the structure of the [(OETPP)Fe(4-MeHIm)$_2$]Cl crystals could not be solved.

All g values of this study and their crystal field parameters are collected in Table 4. It is reassuring to note that all of the values of Δ/λ, also called the Tetragonality of the complex, and a measure of the donor strength of the axial ligand[47−50] are near 2.9−3.3, which is typical of bis-imidazole-coordinated ferrihemes, all of which have $(d_{xy})^2(d_{xz},d_{yz})^3$ electron configurations.[2,3,26,27,47−50]

For those complexes for which the EPR spectra have been recorded on the crystallographically characterized forms, in this and previous studies,[2,4,32,36,53−57] a plot of the largest g value (independent of whether it is a large g_{max} or normal rhombic signal) vs the imidazole (or 4-Me$_2$NPy) dihedral angle provides a fairly linear correlation, Figure 6 (where the g values of the present study are highlighted in color), albeit with some scatter. Magnetic Mössbauer-determined values of the largest hyperfine coupling constant, A_{zz},[37] which should be directly proportional to g_{zz},[58] provide a much more linear correlation for crystalline complexes,[37] but the complexes of the present study have not yet been investigated by magnetic Mössbauer spectroscopy. Nevertheless, it is clear from Figure 6 that there is no break in the value of the largest g value for Type I and Type II[39] complexes, and they can thus be considered as a continuum.

Thus, from consideration of the EPR and crystallographic results for the HIm and N-BzIm complexes of (OETPP)-Fe^{III}, it would appear that the change from normal rhombic to large g_{max} EPR spectral type occurs at ~57° dihedral angle: [(OETPP)Fe(HIm)$_2$]Cl with 57.2° dihedral angle between the axial ligand planes displays a large g_{max} EPR spectrum with g = 3.24 while [(OETPP)Fe(N-BzIm)$_2$]Cl with $\Delta\varphi$ = 56.8° has a normal rhombic EPR spectrum with g_z = 3.08, g_y = 2.19 and unobserved g_x of about 1.31. It should also be noted that the g_{max} value of 3.24 for [(OETPP)Fe(HIm)$_2$]Cl is not much larger than the g_z of

(53) Safo, M. K.; Gupta, G. P.; Walker, F. A.; Scheidt, W. R. *J. Am. Chem. Soc.* **1991**, *113*, 5497−5510.
(54) Roberts, S. A.; Weichsel, A.; Qin, Y.; Shelnutt, J. A.; Walker, F. A.; Montfort, W. R. *Biochemistry* **2001**, *40*, 11327−11337.
(55) Shokhireva, T. Kh.; Smith, K. M.; Berry, R. E.; Shokhirev, N. V.; Balfour, C.; Zhang, H.; Walker, F. A. Manuscript in preparation.
(56) Vinck, E.; Van Doorslaer, S.; Dewilde, S.; Moens, L. *J. Am. Chem. Soc.* **2004**, *126*, 4516−4517.
(57) Kaminskaya, O.; Bratt, P. J.; Evans, M. C. W. *Chem. Phys.* **1995**, *194*, 335−348.
(58) Benda, R.; Schünemann, V.; Trautwein, A. X.; Cai, S.; Polam, J. R.; Watson, C. T.; Shokhireva, T. Kh.; Walker, F. A. *J. Biol. Inorg. Chem.* **2003**, *42*, 787−801.

Table 4. EPR *g* values and Crystal Field Parameters for Model Heme Complexes of This Study

complex	$\Delta\varphi$, deg	g_x	g_y	g_z	Σg^2	V/λ	Δ/λ	V/Δ
Type II Complexes (Normal Rhombic EPR Signals)								
[(OETPP)Fe(HIm)$_2$]Cl from $CDCl_3$/cyclohexane	30.1?[a]	1.63	2.35	2.76	15.82	2.39	2.96	0.81
[(OETPP)Fe(HIm)$_2$]Cl from CD_2Cl_2/dodecane	30.1	1.63	2.35	2.76	15.76	2.39	2.92	0.82
[(OETPP)Fe(N-BzIm)$_2$]Cl major	56.9	1.31[b]	2.19	3.08	16.00	1.49	2.98	0.50
[(OETPP)Fe(N-BzIm)$_2$]Cl minor	–	1.58	2.34	2.79	15.76	2.24	2.86	0.78
[(OETPP)Fe(N-MeIm)$_2$]Cl from$CHCl_3$/cyclohexane, signal 3	44.6[b]	1.18	2.19	3.14	16.00	1.32	2.61	0.51
[(OETPP)Fe(N-MeIm)$_2$]Cl from$CHCl_3$/cyclohexane, signal 4	16.0[b]	1.39	2.20	3.04	16.00	1.60	3.22	0.50
[(OETPP)Fe(N-MeIm)$_2$]Cl from $CHCl_3$/cyclohexane, signal 5	–[b]	1.62	2.36	2.79	15.98	2.33	2.92	0.80
[(OETPP)Fe(N-MeIm)$_2$]Cl from$CHCl_3$/cyclohexane, signal 6	–[b]	2.52	2.35	1.81	14.96	3.63	3.59	1.01
[(OETPP)Fe(4-MeHIm)$_2$]Cl THF, signal 1	–	1.58	2.36	2.82	16.02	2.21	2.88	0.77
[(OETPP)Fe(4-MeHIm)$_2$]Cl THF, signal 2	–	1.71	2.36	2.65	15.52	2.85	2.99	0.95
[(OETPP)Fe(4-MeHIm)$_2$]Cl CD_2Cl_2/dodecane, signal 1	–	1.53	2.27	2.91	15.96	1.94	3.26	0.60
[(OETPP)Fe(4-MeHIm)$_2$]Cl CD_2Cl_2/dodecane, signal 2	–	1.69	2.38	2.69	15.76	2.71	2.88	0.94
Type I Complexes ("large g_{max}" signals)								
[(OETPP)Fe(HIm)$_2$]Cl from $CDCl_3$/cyclohexane	57.2?[a]	–	–	3.17				
[(OETPP)Fe(HIm)$_2$]Cl from CD_2Cl_2/dodecane	57.2	–	–	3.24				
[(OETPP)Fe(N-MeIm)$_2$]Cl from CH_2Cl_2/dodecane, signal 2	59.6	1.20, est.[c]	2.08, est.[c]	3.20	16.01	1.08	3.02	0.36
[(OETPP)Fe(N-MeIm)$_2$]Cl from CH_2Cl_2/dodecane, signal 1	88.1	1.05, est.[c]	2.01, est.[c]	3.30	15.99	1.27	3.23	0.39

[a] Structure obtained on sample crystallized from CD_2Cl_2. [b] Structure obtained on sample crystallized from $CDCl_3$. [c] Calculated from the largest *g* value assuming $\Sigma g^2 = 16.0$ and the tetragonality,[50] $\Delta/\lambda = 3.0-3.3$, as observed for many other bis-imidazole complexes.[2,3,48−50]

3.14 for [(OETPP)Fe(N-MeIm)$_2$]Cl or the g_z of 3.08 for [(OETPP)Fe(N-BzIm)$_2$]Cl.

Earlier we reported the structure of the [(OETPP)Fe(4-Me_2NPy)$_2$]$^+$ complex with 70.0° dihedral angle and large g_{max} EPR signal, $g_{max} = 3.29$.[32] Recently, Nakamura and coworkers[59] published the structure of a different polymorph of [(OETPP)Fe(4-Me_2NPy)$_2$]$^+$ with an intermediate dihedral angle, $\Delta\varphi = 53.2°$.[59] This angle is only slightly smaller than the $\Delta\varphi$ angles of the [(OETPP)Fe(N-BzIm)$_2$]$^+$ (56.8°) and one molecule of the [(OETPP)Fe(HIm)$_2$]$^+$ complex (57.2°) from the present work. Interestingly, although not published in the paper,[59] like [(OETPP)Fe(N-BzIm)$_2$]$^+$ (56.8°) of the present study, [(OETPP)Fe(4-Me_2NPy)$_2$]$^+$ (53.2°) has a normal rhombic EPR signal, with $g_z = 3.06$, $g_y = 2.16$, and $g_x = 1.40$,[60] thus confirming that the changeover from normal rhombic to large g_{max} EPR signal type occurs at $\Delta\varphi$ larger than the 53.2−56.8° range. The $\Delta\varphi$ and g_{zz} values of this complex are included in Figure 6.

On the basis of this and previous studies, the EPR signal type of model hemes appears to change from large g_{max} to normal rhombic at ∼57° with continuous change in the largest *g* value upon continuous change of the angle between the axial ligand planes from 90° to 0° (albeit with some scatter). While this value may appear to be a very sharp transition because of the 56.8° and 57.2° angles of this study, that is undoubtedly a result of the limited number of complexes having ligand plane dihedral angles close to 57°, and thus the transition from large g_{max} to normal rhombic may not occur at exactly that angle for other complexes. For example, recently the *rhombic* EPR spectra of mouse neuroglobin and human cytoglobin in frozen aqueous solution have been reported to have $g_z = 3.10$ and 3.20, respectively,[56] values somewhat larger than have been seen previously for relatively sharp rhombic signals of low-spin ferriheme centers having three well-resolved EPR spectral features. The crystal structures of those two proteins have been reported and have $\Delta\varphi = 59°$ [61] and 60°,[62,63] respectively, which may suggest *either* that the angle at which the spectral type changes from normal rhombic to large g_{max} may be more flexible than suggested by the model ferriheme complexes studied in this work *or* that the $\Delta\varphi$ value of the frozen solution samples of these proteins is somewhat different from that observed in the crystalline state. Further studies of these six-coordinate bis-histidine heme proteins may clarify this point in the future. Certainly, the solution NMR spectra of mouse neuroglobin[64] indicate a much smaller value of $\Delta\varphi$ (∼15−20°)[65] than that observed in the crystal structure.[61] At present, we can simply conclude that the value of $g_z = 3.14$ for 45% of the molecules in the N-MeIm complex used for simulating the EPR spectrum shown in Supporting Information Figure S5 is not inordinately large for a normal rhombic EPR signal.

It should also be noted that the *g* values observed for the mitochondrial cytochrome bc_1 complex hemes b_H and b_L[8,9,12−14,16,17,19,20,25,26−29] are larger than those of model heme complexes and small heme proteins,[54−57,61−63] including the bis-histidine-bound heme of the membrane-bound cytochrome *c* subunit of *Rhodopseudomonas viridis* reaction centers ($g = 3.31$, $\Delta\varphi = 64°$),[57] of the same dihedral angle as heme b_L, also shown in Figure 6. The reason(s) for these larger *g* values for the large g_{max} EPR signals of the membrane-bound cytochrome *b* proteins of the bc_1 complex is not known at present, although we have speculated that it may be in part a result of the fact that the electrostatic surroundings of the heme centers in the concentrated crystals of the model heme complexes is very different from that in the membrane-bound cytochromes *b*,[37] and also that the

(59) Ohgo, Y.; Ikeue, T.; Takahashi, M.; Takeda, M.; Nakamura, M. *Eur. J. Inorg. Chem.* **2004**, 798−809.
(60) Nakamura, M. Personal communication.
(61) Vallone, B.; Nienhaus, K.; Brunori, M.; Nienhaus, G. U. *Proteins: Struct. Func. Bioinf.* **2004**, *56*, 85−94.
(62) de Sanctis, D.; Dewilde S.; Pesce, A.; Moens, L.; Ascenzi, P.; Hankeln, T.; Burmester, T.; Bolognesi, M. *J. Mol. Biol.* **2004**, *336*, 917−927.
(63) Sugimoto, H.; Makino, M.; Sawai, H.; Kawada, N.; Yoshizato, K.; Shiro, Y. *J. Mol. Biol.* **2004**, *339*, 873−885.
(64) Du, W.; Syvitski, R.; Dewilde, S.; Moens, L.; La Mar, G. N. *J. Am. Chem. Soc.* **2003**, *125*, 8080−8081.
(65) Walker, F. A. *J. Biol. Inorg. Chem.* **2006**, *11*, 391−397.

smallest Fe−Fe distances in the cytochrome bc_1 complex are about 20 Å, while the smallest Fe−Fe distance in the crystals of the model heme complexes of this study is 12.1−12.3 Å. Although the latter distances are large enough that no electron spin−spin splitting of the EPR spectra is expected, we have pointed out elsewhere that it is not presently known whether there may be a bulk electrostatic effect on the observed g values.[37] It should also be mentioned that the deviation of heme b_L ($g_{max} \approx 3.75-3.78$, $\Delta\varphi = 84.4° \pm 3.2°$) from the average correlation line for the model hemes is actually greater than that of heme b_H ($g_{max} \approx 3.41-3.60$, $\Delta\varphi \sim 59.5° \pm 7.1°$). Heme b_L is the one that has one histidine ligand (H82 or H83, depending on species) acting as a N−H hydrogen-bond donor to a conserved threonine (T46, T47, or T62, depending on species) side chain oxygen, and it is possible that the exact orientation that this hydrogen-bond interaction brings about results in an additional contribution to the g value of this species; certainly the heme b_L EPR signal is unusually sharp for a large g_{max} signal and unusually strongly ramp-shaped,[26−29] indicating that there is something unique about it.

In conclusion, we have shown that there is a rough correlation between axial ligand plane dihedral angle and the value of the largest g value for low-spin ferriheme complexes having both normal rhombic and large g_{max} EPR signals and that there is no break in this plot between complexes with these two types of EPR signals. Furthermore, the dihedral angle at which the signal type changes from large g_{max} to normal rhombic (Type I to Type II)[39] is $\sim 57°$, probably with a range of $\pm 3-5°$ or so. Factors other than the axial ligand plane dihedral angle, including the quality of the crystalline sample, the choice of the types of complexes (those that must be saddled vs those that need not be saddled), and other properties of the sample that could lead to microheterogeneity (such as solvent content and disorder, etc.), probably affect the exact value.

Acknowledgment. The support of this research by the National Institutes of Health, Grant No. DK-31038 (F.A.W.), the National Science Foundation (Grant No. CHE-9610374 for the X-ray diffractometer), and the University of Arizona Molecular Structure Laboratory is gratefully acknowledged. We thank Dr. Robert E. Berry and Dr. Andrei V. Astashkin for their help with EPR experiments and Dr. Mikio Nakamura for providing the EPR spectrum of his crystalline complex of [(OETPP)Fe(4-Me_2NPy)$_2$]ClO_4. This paper is dedicated to Professor Alfred X. Trautwein on the occasion of his 65th birthday.

Supporting Information Available: Details of the structure determinations, Figure S1 − a reciprocal lattice view of the reflection array, for [(OETPP)Fe(HIm)$_2$]Cl; Figure S2 − overlay of porphyrin cores of the two independent molecules of [(OETPP)-Fe(HIm)$_2$]Cl; Figure S3 − thermal ellipsoid diagrams for the two molecules of [(OETPP)Fe(HIm)$_2$]Cl; Figure S4 − thermal ellipsoid diagrams for [(OETPP)Fe(N-BzIm)$_2$]Cl; Figure S5 − simulation of the EPR spectrum of crushed crystals of [(OETPP)Fe(N-MeIm)$_2$]-Cl; Tables S1−S5, atomic coordinates and equivalent isotropic displacement parameters; bond lengths and angles; anisotropic displacement parameters; hydrogen coordinates and isotropic displacement parameters; torsion angles for [(OETPP)Fe(HIm)$_2$]-Cl. Tables S6−S10 and S11−S15 − the same for [(OETPP)Fe-(N-MeIm)$_2$]Cl and [(OETPP)Fe(N-BzIm)$_2$]Cl, respectively (65 pages). This material is available free of charge via the Internet at http://pubs.acs.org.

IC060283H